Solar Energy Materials & Solar Cells 94 (2010) 114–127

Contents lists available at ScienceDirect

Solar Energy Materials & Solar Cells

journal homepage: www.elsevier.com/locate/solmat

Review

Polymer solar cells: Recent development and possible routes for improvement in the performance

Wanzhu Cai, Xiong Gong *[,1], Yong Cao

Institute of Polymer Optoelectronic Materials and Devices, Key Laboratory of Specially Functional Materials, Ministry of Education, South China University of Technology, Guangzhou 510640, PR China

ARTICLE INFO

Article history:
Received 11 May 2009
Received in revised form
1 October 2009
Accepted 2 October 2009
Available online 3 November 2009

Keywords:
Polymer solar cells
Power conversion efficiency
Stability
Manufacturing process

ABSTRACT

The development of polymer solar cells is rapidly accelerating as the need of new clean energy sources. Polymer solar cells are attractive because they can be manufactured on plastic substrates by a variety of printing techniques. In this article, we provided an overview on basic operational principles and recent development of polymer solar cells. The possible routes for improvement in power conversion efficiency, stability, and the effects toward manufacturing of polymer solar cells were summarized and highlighted.

Contents

1. Introduction

Polymer solar cells have certain attractive features [1]. Because the active materials used for fabrication devices are soluble in most of common organic solvents, polymer solar cells have potentials to be flexible and to be manufactured in a continuous printing process like printing newspapers. Various printing and coating technologies have been proven their compatibility with semiconducting polymer processing [2]. Fig. 1 illustrated that polymer solar cells can be manufactured using standard printing processes [3].

Power conversion efficiency (PCE) beyond 6% [4,5] was reported recently, but this value is far away for daily applications. Deep investigation of operating mechanism and creative synthesis

* Corresponding author.
E-mail address: xgong@physics.ucsb.edu (X. Gong).
[1] *Current address*: Center for Polymers and Organic Solids, University of California, Santa Barbara, USA.

0927-0248/$ - see front matter © 2009 Elsevier B.V. All rights reserved.
doi:10.1016/j.solmat.2009.10.005

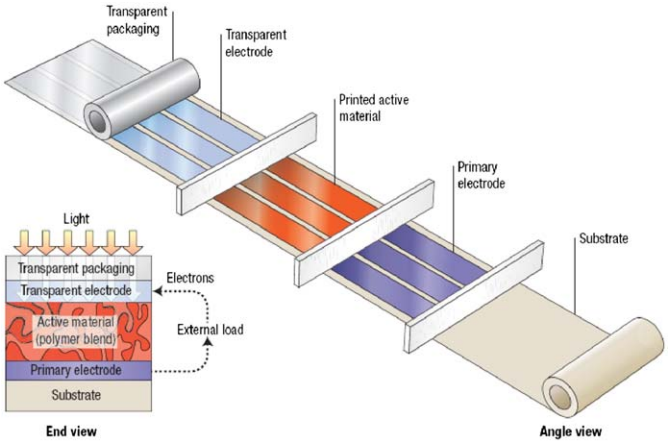

Fig. 1. Schemtic illustration of polymer solar cells can be manufactured by standard printing rocesses [3].

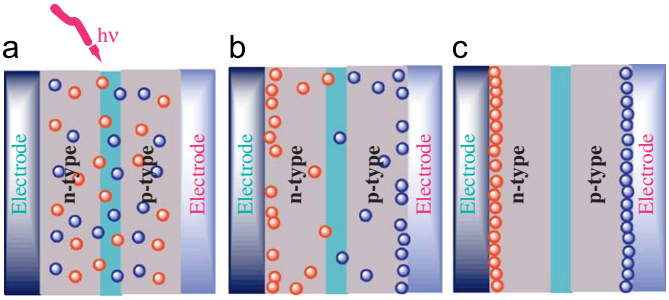

Fig. 2. Schematic illustration of operational mechanisms in polymer solar cells. (a) Absorption of light, (b) charge separation and (c) charge collection.

of novel materials for approaching high performance polymer solar cells are summarized in the literature [6]. Improving PCE is the first aim of the current investigation. At the same time, some visionary scientists have already paid their attention to the lifetime of these flexible solar cells [7]. So far the best lifetime reported by Konarka Technology was more than one year [8].

This article overviewed recent development of polymer solar cells and discussed the possible routes for improvement in the performance of polymer solar cells. We started with an introduction of basic operational principles and polymer solar cells materials. We highlighted current most prominent materials system, a mixture of poly(3-hexylthiophene) (P3HT):1-(3-methoxyxarbonyl) propyl-1-phenyl [6,6] C_{61} ($PC_{60}BM$). The recent development in polymer solar cells is summarized in Section 3. In Section 4, we discussed the possible routes for improvement in the performance of polymer solar cells, i.e. improving absorption, enlarging open circuit voltage, towards a controllable morphology, using new device structures. We also discussed the stability of polymer solar cells, ITO-free solar cells and the effects toward to manufacturing polymer solar cells. We finished this article with conclusion and outlook.

2. Operational principles

The process of conversion of light into electricity by polymer solar cells can be illustrated in Fig. 2. There are three operational mechanisms determined that polymer solar cells have capability to generate electricity: absorption of a photon either by electron donor and/or electron acceptor, leading to the formation of an excited state, that is, the bound electron–hole pairs creation; exciton diffusion at the interface between the electron donor and

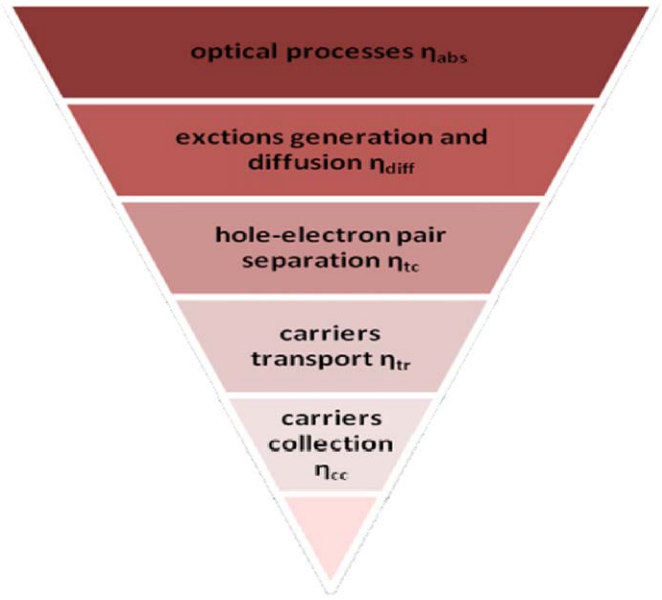

Fig. 3. Schematic illustration of energy transfer efficiencies in polymer solar cells.

the electron acceptor, that is, charge separation occurs and charge transport within the polymer blend to the respective electrodes.

The *PCE* of solar cell is defined as

$$PCE = \frac{J_{sc} V_{oc} FF}{P_{in}} \tag{1}$$

where J_{SC} is the short circuit current, V_{OC} is the open circuit voltage, *FF* is the fill factor and P_{in} is the incident light power which is standardized as 100 mW/cm^2.

J_{SC} can be obtained by

$$J_{sc} = \frac{q}{\hbar c} \int_{\lambda_{min}}^{\lambda_{max}} EQE P_{in}(\lambda) \lambda \, d\lambda \tag{2}$$

where q is the elementary charge, $\hbar$ is Planck constant, C is the speed of light and *EQE* is the external quantum efficiency, which is the ratio of output electrons to the incident photons. *EQE* is equal to the multiplication of all the efficiencies in the energy transfer processes.

$$EQE = \eta_{abs} \eta_{diff} \eta_{tc} \eta_{tr} \eta_{cc} \tag{3}$$

where η_{abs} is the photon absorption efficiency. The last four parameters, namely η_{diff}, η_{tc}, η_{tr} and η_{cc}, are the internal quantum efficiency (IQE), which represents the efficiencies of the exciton diffusion process, the hole–electron separation process, the carrier transport process and the charge collection process, respectively. The energy transfer process efficiencies in the solar cells can be described in Fig. 3.

The most effective way to improve the J_{SC} is to enlarge η_{abs}. In the standard solar spectrum (AM 1.5 G), the maximum irradiance energy is at ~500 nm, the maximum photon flux is at ~670 nm. Therefore, polymer solar cells materials need not only to absorb the photons at the maximum irradiance but also to have a broad absorption spectrum and high absorption coefficient.

Semiconducting polymers have lower dielectric constant than that of inorganic semiconductors. The electrostatic attractive force between the holes and the electrons, coulomb attraction, is proportional to $1/\varepsilon$, $\varepsilon \approx 3$ [9] (typical values for semiconducting polymers). The coulomb attraction in inorganic semiconductors with a larger dielectric constant can be neglected. In contrary, semiconducting polymers require a force more than 0.4 eV [10] to separate the exciton. The split area is at the interface between

electron donor and electron acceptor. The difference between the lowest unoccupied molecular orbital (LUMO) energy level of these two types of materials is the headstream of charge carriers.

Semiconducting polymers have higher extinction constant than that of inorganic photovoltaic materials. About 300 nm film is thick enough to absorb the most incident light [11]. But due to the low carrier mobility, the optimized thickness for most polymer solar cells is less than 100 nm [12,13]. Polymer solar cells with a new device configuration were built for absorbing more photon and improving charge carrier mobility [14,15].

When a photon was absorbed by an electron donor, the electron was excited to an exciton energy state which was inside the energy gap. The electron binds with the hole with a binding energy of 0.4 eV, and this quasi-particle will diffuse in its lifetime until it is recombined and/or separated. The typical exciton diffusion length in semiconducting polymers is less than 20 nm [12]. If the exciton does not separate in time, it will recombine to a photon, or decay via thermalization. η_{diff} in Eq. (3) represents the efficiency of the exactions diffusion to the separation point.

When the exciton meets at the interface between electron acceptor with high electronic affinity and electron donor with high ionization energy, it will be separated in the time scale of femto-second (~50 fs) [16]. This process is much faster than other competition processes like photoluminescence (ns) and charge recombination (μs). As a result, η_{tc} is approximately 100%. But geminate polaron pairs are photo-induced instead of exciton, which are not separated at the interface between the electron donor and the electron acceptor. Because the intrinsic characteristic of polymer molecules, high traps density, dead end in the transport net and so on, the mobility is low and unbalanced [17].

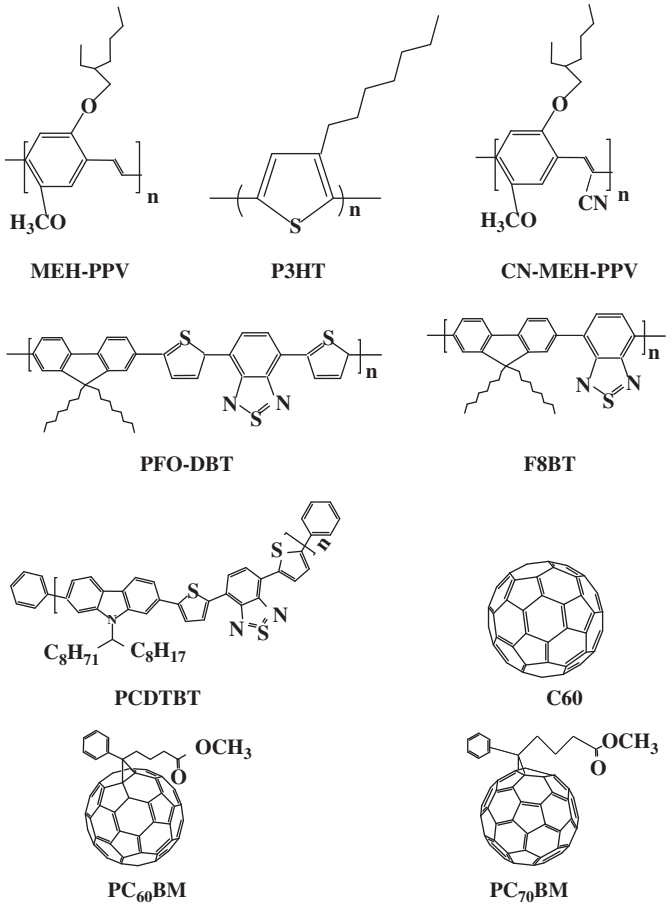

Fig. 4. Example of organic semiconductors used in polymer solar cells.

Therefore, the charge transport efficiency η_{tr} in polymer solar cells is not a unit. Due to an ohm contact between active layer and the electrodes and an enlarged build-in electric field, a better charge transport condition was created, as a result, charge transport efficiency was compromised [18,19].

The work function of the electrode is pinning to the corresponding material energy level. V_{OC} of bulk heterojunction cells is directly related to the energy difference between the highest occupied molecular orbital (HOMO) level of the electron donors and the LUMO level of the electron acceptors [20]. V_{OC} is empirically described by following formula [21]:

$$eV_{OC} = \left(\left|E_{HOMO}^{Donor}\right| - \left|E_{LUMO}^{Acceptor}\right|\right) - 0.3 \quad (4)$$

3. Recent development of polymer solar cells

3.1. Polymer solar cells materials

Generally, organic materials having delocalized π electrons, absorbing sunlight, creating photo generated charge carriers and transporting these charge carriers can be used for fabrication of polymer solar cells. These materials are classified to the electron donors and the electron acceptors.

Most of semiconducting polymers are hole-conductors. This kind of semiconducting polymers was named as the electron donor polymers. Fig. 4 shows some representative semiconducting polymers. Four important representatives of electron donor polymers are MEH-PPV, P3HT, PFO-DBT [22] and PCDTBT [23]. There are number of excellent in-depth reviews covering materials selection for polymer solar cells [12,24,25]. Low bandgap polymers and polymer precursors were also under the investigation for polymer solar cells [26–30].

The electron acceptor polymers like CN-MEH-PPV, F8TB, and small molecules, C_{60} and soluble derivatives of C_{60} and C_{70}, namely $PC_{60}BM$ and $PC_{70}BM$, are also shown in Fig. 4. Fullerenes are considered to be the best electron acceptors so far. This is because: (i) ultrafast (~50 fs) photo induced charge transfer was happened between the donor polymers and fullerenes; (ii) fullerenes exhibited high mobility, for example, $PC_{60}BM$ shown electron mobility up to 1 $cm^2\,V^{-1}\,s^{-1}$ [31] measured by field effect transistors; (iii) fullerenes shown a better phase segregation in the blend film.

The full names of above representative organic materials are:

MEH-PPV: poly [2-methoxy-5-(2'-ethyl-hexyloxy)-1,4-phenylene vinylene]P3HT: poly(3-hexylthiophene)
PFO-DBT: poly [2,7-(9,9-dioctyl-fluorene)-alt-5,5-(4,7'-di-2-thienyl-2', 1', 3'-benzothiadiazole)
PCDTBT:poly[N-9'-hepta-decanyl-2,7-carbazole-alt-5,5-(4',7'-di-thienyl-2'1',3'-b3nzothiadizaole)
CN-MEH-PPV:poly-[2-methoxy-5,2'-ethylhexyloxy]-1,4-(1-cyanovinylene)-phenylene
F8TB:poly(9,9'-dioctylfluorene-co-bis-N,N'-(4-butylphenyl)-bis-N,N'-phenyl-1,4-phenylenediamine
$PC_{60}BM$: 6,6-phenyl-C61-butyric acid methyl ester
$PC_{70}BM$: 6,6-phenyl-C71-butyric acid methyl ester

3.2. The P3HT:PCBM blend

In the past years, P3HT was a prominent semiconducting polymer in polymer solar cells. Easy to self-assemble is the advantage of P3HT [32]. Thermal annealing under the tempera-

ture above its glass transition temperature can improve J_{SC} and *FF* significantly, thus resulting in higher *PCE* [33]. The enhancement is probably due to the better organization of P3HT molecules [34]. X-ray diffraction demonstrated that part of P3HT molecules are oriented with their main chain parallel to and side chains perpendicular to the substrate [35]. Fig. 5 illustrated the molecular structure was near the interface before and after thermal annealing treatment [36]. Increase in the hole mobility in the P3HT phase in the blend from annealed devices is an important factor which result in an improved *PCE*. The hole mobility is dramatically increased by more than three orders of magnitude, up to $4.4\times10^{-2}\ cm^2\ V^{-1}\ s^{-1}$ was observed [37–39]. Other contributions for enhancement in the performance were strong red-shift of the absorption [37], reduced recombination [39], low compositions ratio of $PC_{60}BM$ [40].

Blom et al. deduced that an enhanced EQE under short circuit condition was probably due to 90% dissociation ratio of the electron–hole pair close to the interface between the electron donor and the electron acceptor [37]. By using transient absorption spectroscopy, Clarke and colleagues [41] found that a charge photo generation yield is significant enhanced in the time scales of microsecond which is a greater time scales than one of exciton splitting. It was also found that the ionization potential of P3HT was decreased after thermal annealing. By using ultrafast time-resolved spectroscopy, Hwang et al. [42] found that thermal annealing of P3HT:PCBM films resulted in a shorter lifetime of the bound radical pair state. This finding was in good agreement with that an offset of lower LUMO level is corresponding to a lower bandgap of P3HT [41].

It was also found that the performance of P3HT:PCBM solar cells were affected by molecular weights, polydispersity [43], regiochemistry [44], mixed solvents without heat treatment [45], applying external electric field [46], proper solvent [47], solvent-vapor treatment [48], adding additives liking oleic acid [49]. All these results indicated that it was very complex to control the film morphology.

In conclusion, P3HT:PCBM devices were well investigated. It was clearly that P3HT:PCBM was not a proper system for approaching high-performance because the bandgap of P3HT (1.85 eV) is too large. This bandgap only matches 46% of solar irradiance spectrum. Supposing EQE from P3HT:PCBM device is 100% and a maximum J_{SC} is 18.7 mA cm^{-2} [50], *FF* is 65%, V_{OC} is 0.6 V, the projected maximum *PCE* is 7.2%. This value is far below the targeted *PCE*.

3.3. Recent development

The development in polymer solar cells is very fast. The PCE of 6% from single active layer polymer solar cells was reported recently [4,5]. Table 1 summarized the best performances of polymer solar cells. Polymer-fullerene solar cells have significant high performance among others.

4. Possible routes for improving the performance

4.1. Improving absorption

One of the limited parameters in polymer solar cells was poor absorption. Large band gap materials own a mismatch to the terrestrial solar spectrum. For example, poly (*p*-phenylene vinylenes) (PPVs) and polythiophenes, their bandgaps are ~1.85 and ~2.2 eV. The bandgap of 1.85 eV (absorb edge was at 670 nm) only allowed 46% of photon was harvested. A bandgap of 1.1 eV (Si) allowed more than 90% of photon was harvested. The optical loss due to polymer band gap mismatched with the solar spectrum was shown in Fig. 6.

In order to exceed PCE over 10% from single layer polymer solar cells, the bandgap of donor polymers should be ~1.7 eV and the LUMO of this donor polymers should be ~−3.9 eV if PCBM is

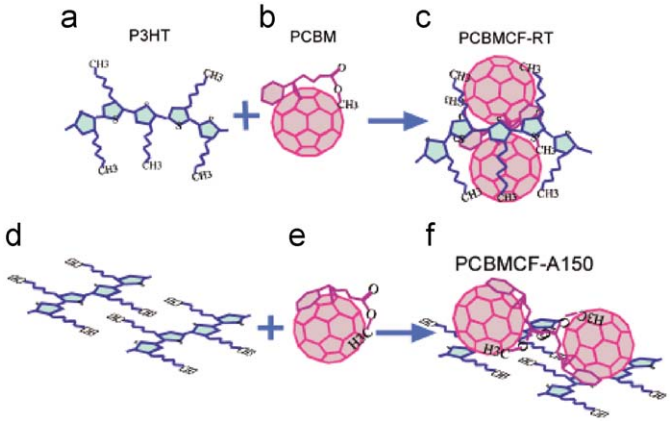

Fig. 5. Illustrations of the molecular structure near the interface before (a–c) and after (d–f) annealing [36].

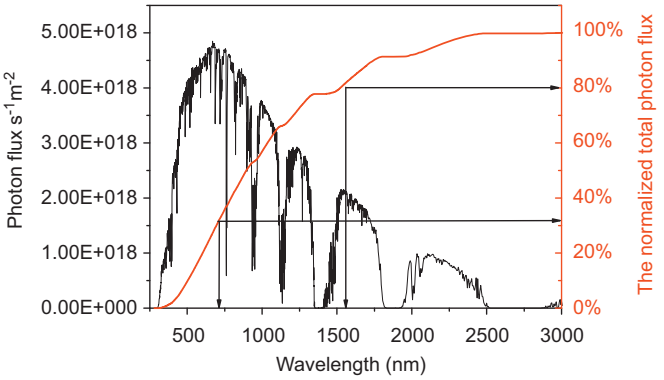

Fig. 6. Optical losses due to polymer band gap mismatch with solar spectrum.

Table 1
A summary of recent development in polymer solar cells.

PCE (%)	V_{OC} (V)	FF (%)	J_{SC} (mA/cm^2)	Active materials	Ref.
~5	~0.6	~60	~11	P3HT:PCBMs	[14,46,49]
5.4	0.9	50.7	9.5	PSiF-DBT:PCBM	[51]
5.3	0.56	63.3	15	PTB1:P_{71}CBM	[13]
5.2	0.62	55	16.2	PCPDTBT:PCBM	[52]
4.76	0.58	65.4	12.5	PTB1:PCBM	[13]
2.18	~0.6	~50	~7	Hyperbranched CdSe nanoparticle:P3HT	[53]
2.8	0.76	40	9.1	OC_1C_{10}-PPV:CdSe tetrapods	[54]
6.5	1.24	67	7.8	PCPDTBT:PCBM/TiO_x/PEDOT:PSS/P3HT:PCBM	[55]
6	0.88	66	10.6	PCDTBT:PC_{70}BM/TiO_x	[4]

Table 2
Performance of polymer solar cells with optical spacer.

Active layer	Optical spacer		PCE (%)	V_{OC} (V)	J_{SC} (mA/cm^2)	FF (%)	Ref.
Thickness (nm)	Materials	Thickness (nm)					
P3HT:PCBM			2.3	0.51	7.5	54	[14]
100	TiO_x	30	5	0.61	11.1	66	
P3HT:PCBM			4.0	0.62	10.7	60	[66]
200	TiO_x	35	4.1	0.62	10.8	61	
P3HT:PCBM			~3.1	~0.58	~9.0	~64	[67]
100	TiO_x	20	3.9	0.58	11.52	58	
P3HT:PCBM			3.95	0.65	10.61	57.1	[68]
100	CuPc	8	4.13	0.64	12.54	51.1	

Table 3a
The performance of polymer solar cells with an n-type buffer layer.

Active layer	Buffer layer		J_{SC} (mA/cm^2)	V_{OC} (V)	FF (%)	PCE (%)	Ref.
	layer	d (nm)					
m-MTD ATA /Nd(DBM)$_3$bath/LiF	LiF	0	0.081	1.69	31	1.1	[85]
	LiF	0.6	0.145	1.96	32	2.2	
MDMO-PPV/PCBM/LiF	LiF	0		0.759	53		[86]
	LiF	1.2		0.832	61.1		
MDMO-PPV/PCBM/SiO_x	SiO_x	0		0.759	53		
	SiO_x	1.2		0.796	lower		
MDMO-PPV/PCBM/LiF	LiF	0		0.62	51		
	LiF	~		0.763	54		
PEDOT:PSS/P3HT:PCBM/LiF	LiF	0	8.38	0.49	52		[87]
	LiF	~	8.07	0.57	63		
PEDOT:PSS/P3HT:PCBM/CaO	CaO	0	8.38	0.49	52		
	CaO	~	8.53	0.57	59	2.85	
PEDOT:PSS/P3HT:PCBM/TiO_x	TiO_x	0	10.7	0.62	60	4.0	[66]
	TiO_x	35	10.8	0.62	61	4.1	
PEDOT:PSS/P3HT:PCBM/Cs_2CO_3	Cs_2CO_3	0				2.3	[88]
	Cs_2CO_3	~				3.1	
PEDOT:PSS/P3HT:PCBM/Pentacene	Pentacene	0	7.61	0.61	43.19	2	[89]
	Pentacene	1	9.56	0.63	51.3	3.09	
PEDOT:PSS/P3HT:PCBM/TiO_x	TiO_x	0	7.5	0.51	54	2.3	[14]
	TiO_x	30	11.1	0.61	66	5	
	TiO_x	5		0.6	70	4.05	[90]
PEDOT:PSS/P3HT:PCBM/F-PCBM	F-PCBM	0	8.72	0.55	64	3.09	[91]
	F-PCBM	2	9.51	0.57	70	3.70	

used as the electron acceptor [21]. The discussion of band alignment in details was summarized in the literatures [50,56]. The current state-of-art approaches to realize these low bandgap donor polymers are based on donor–acceptor molecule structures. The strategy for synthesizing these polymers is often selecting donor unit with high ionization potential and acceptor unit with high electron affinity. Recent developments in organic materials for photovoltaic applications are summarized in literatures [57,58].

Another approach to realize polymer blending system covering wide absorption region is to have new electron acceptors whose absorption covers wide region. $PC_{71}BM$ [59] and $PC_{85}BM$ [60] are reported to have better absorption in the visible region, but they were worse miscibility to the donor polymers. Fullerenes derivative, endohedral fullerenes, $Lu_3N@C_{80}$-PCBM [61] was anticipated to have higher PCE from P3HT:$Lu_3N@C_{80}$-PCBM solar cells because $Lu_3N@C_{80}$-PCBM has similar characteristics in solubility and miscibility as $PC_{60}BM$ has, but more negative LUMO than that of $PC_{60}BM$. A new electron acceptor (99'BF) which gives a open circuit voltage of 1.20 V from polymer solar cells made by P3HT blended with 99'BF was under the investigation at the University of California, Santa Barbara [62,63].

Increasing the miscibility of the electron acceptor composition, decreasing the ratio of electron donor to electron acceptor, can improve the optical density. Inorganic nano-material with high mobility and better absorption than fullerene is another good alternative [64]. But the drawback was photo current has to transport across the surfactant which coated on the surface of nanoparticles, resulting in a limited transporting of photo-induced current from the blend of semiconducting polymer with inorganic nanopartices. However, surfactant is certainly necessary for the dispersion of nanopartices into in the organics solvent, giving a uniform thin film from the solution containing semiconducting polymer and inorganic nanoparticles [65].

Introducing an optical spacer into the devices is another approach to increase the total thickness of active layer. The thickness of the device with an optical spacer is not good enough to trap all the incident photons. But, the light intensity inside the device was spatially redistribution due to optical interference effect. A better light intensity distribution formed by optical spacer will result in a high performance of polymer solar cells [14]. Table 2 summarizes the performance of polymer solar cells with an optical spacer.

Table 3b
The performance of polymer solar cells with a p-type buffer layer.

Active layer	Buffer layer		J_{SC}(mA/cm^2)	V_{OC}(V)	FF(%)	PCE(%)	Ref.
	layer	d(nm)					
PEDOT:DSS/a-PANINs/P3HT:PCBM	PANIN	0	8.83	0.64	55	3.39	[92]
	PANIN	~	10.96	0.64	60	4.26	
TFB:TPDSi$_2$/MDMO:PPV:PCBM	TFB:TPDSi$_2$	0	4.56	0.74	43.4	1.46	[93]
	TFB:TPDSi$_2$	10	4.62	0.89	54.4	2.29	
Gold nanoparticle (GNPs)/P3HT:PCBM	GNPs	0	5.29	0.58	57	2.07	[94]
	GNPs	~	6.15	0.54	57	2.21	
V_2O_5/P3HT:PCBM	V_2O_5	0	8.95	0.59	59.6	3.18	[95]
	V_2O_5	3	8.83	0.59	59.1	3.10	
MoO_3/P3HT:PCBM/Al	MoO_3	0	8.95	0.59	59.6	3.18	
	MoO_3	5	8.94	0.60	61.9	3.33	
PEDOT:PSS/CuPc/P3HT:PCBM	CuPc	0	10.61	0.65	57.1	3.95	[68]
	CuPc	8	12.54	0.64	51.1	4.13	
AgO_x/PEDOT:PSS/P3HT:PCBM	AgO_x	0	10.8	0.61	66	4.4	[96]
	AgO_x	~	12.7	0.60	63	4.8	
PEDOT:PSS/SWNT/P3HT:PCBM	SWNT	0	21.6	0.51	47	4	[97]
	SWNT	~	21.0	0.59	51	4.9	
SWNT/PEDOT:PSS/P3HT:PCBM	SWNT	0	21.6	0.51	47	4	
	SWNT	~	24.1	0.59	44	4.9	

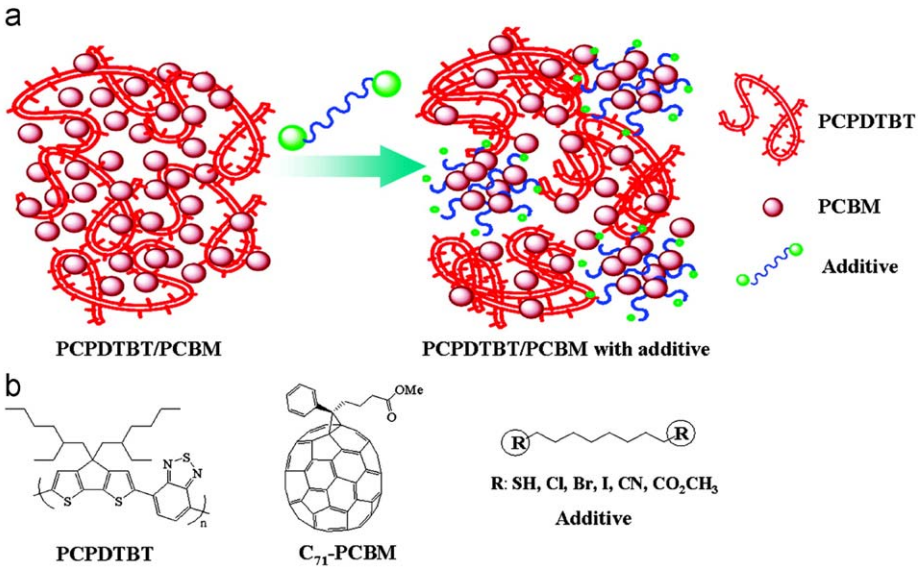

Fig. 7. Schematic depiction of the role of the processing additive in the self-assembly of bulk heterojunction blend materials [111].

Optical spacer does not always bring the observable improvement in *PCE*. The enhancement by the optical spacer is smaller than we expected. As the weak electrical transport and the poor carrier collection, the contribution absorption by the optical spacer will be reduced. In addition, a rough surface of the active layer will be reduced by an optical spacer [66].

It noted that the thickness of the active layer is limited due to the low carrier mobility of semiconducting polymers. As a result, the optical absorption coefficient of semiconducting polymers is not big enough and a lot of part photon flux was lost.

The major losses in polymer solar cells are the sub-band-gap transmission and the thermalization of the hot charge carriers [69]. The tandem architecture can circumvent above effects simultaneously. The V_{OC} will be the sum of the individual cells and the *FF* will be properly unchanged along with increasing thickness of devices. The top cells with low bandgap and the bottom cells with large bandgap are in series at the interface with recombination center function. The average of optical density will increase as the tandem cells harvest broad fraction of solar emission spectrum. Organic tandem cells were firstly fabricated by organic small molecules [70]. Evaporation processing is an easy way to fabricate multilayer structure with a sharp interface between the layers, but the limitation is it will be extremely expensive to make large size because the huge cost in making big deposition system. Using orthogonal solvents is one of the approaches to realize multilayer structure by solution processing, but it is difficult to get a sharp interface. Krebs with colleagues [71] have used the materials with thermoclevable properties to fabricated tandem cells by solution processing. After thermal treatment, the film processed by spin-coating from corresponding solutions will convert to an insoluble state to the solvent used for processing following layer. The device exhibited operational stability in air without any encapsulation. All solution processed bulk heterojunction tandem cells were firstly reported by Gilot and colleagues [72]. The inter layer was combined with a UV illumination treated ZnO nanoparticle with neutral PH PEDOT. V_{OC} of a triple junction solar cell was reached to 2.19 V which was corresponded to the sum of V_{OC} from individual single cells. The

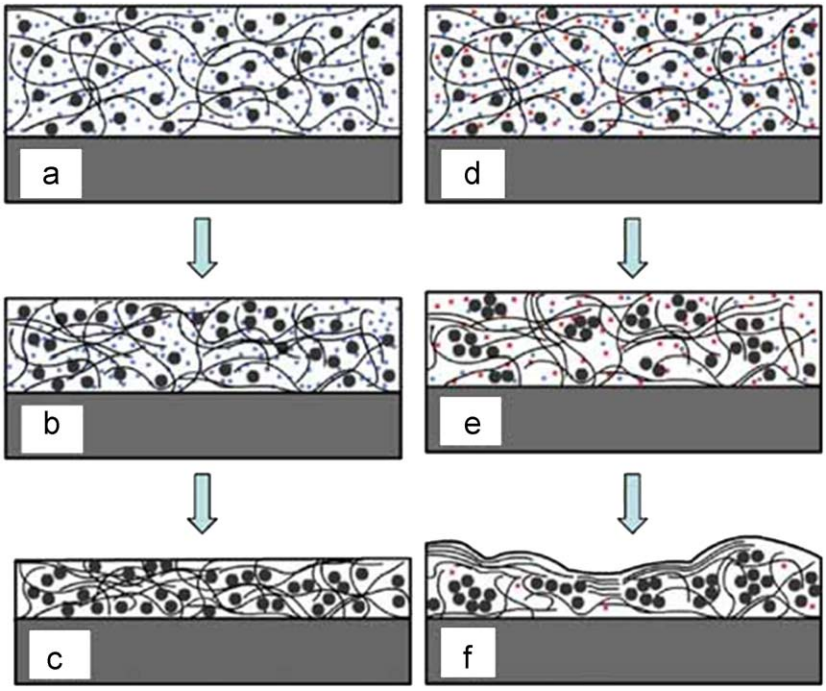

Fig. 8. Proposed model during spin-coating process. Black wire: P3HT polymer chain; Big black dots: PCBM; blue dots: DCB molecules and red dots: 1,8-octanedithiol molecules. (a–c) Correspond to three stages in the spin-coating process when DCB is the sole solvent; (d–f) correspond to three stages in the spin-coating process when octanedithiol is added in DCB. Note the difference of PCBM distribution in the final stage of each case, (c) and (f). The total numbers of big black dots are same in all the images [112].

Table 4
Performance of polymer solar cells with an inverted structure.

Structure	PCE (%)	J_{SC} (mA/cm^2)	V_{OC} (V)	FF (%)	Ref.
ITO/nano-TiO_2/P3HT:PCBM/V_2O_5/Al	2.71	0.59	10.96	42	[114]
ITO/Cs_2CO_3/P3HT:PCBM/V_2O_5/Al	2.25	0.56	8.42	62.1	[113]
	4.2	0.59	11.22	47.5	[115]
ITO/TiO_x/P3HT:PCBM/PEDOT:PSS/Al	3–3.5	0.57–0.56	10–8.6	63–63	[11]
ITO/ZnO/P3HT:PCBM/Ag	2.97	0.556	11.22	47.5	[116]
ITO/TiO_x/P3HT:PCBM/PEDOT:PSS/Au	3.1	0.56	9.0	62	[117]
ITO/TiO_x/SAM/P3HT:PCBM/PEDOT:PSS/Al	3.8	0.62	10.6	57.2	[118]
ITO/nc-TiO_2/P3HT:PCBM/MoO_3/Ag	2.57	0.628	6.57	62.3	[119]
ITO/nano-ZnO/P3HT:PCBM/VOx/Ags	3.9	0.58 V	10.4	65	[15]
ITO/nano-ZnO/P3HT:PCBM/Ag	2.7	0.57	9.6	50	[120]
ITO/ZnO-NP/P3HT:PCBM/PEDOT:PSS/Ag	3.61	0.623	10.69	54.2	[121]

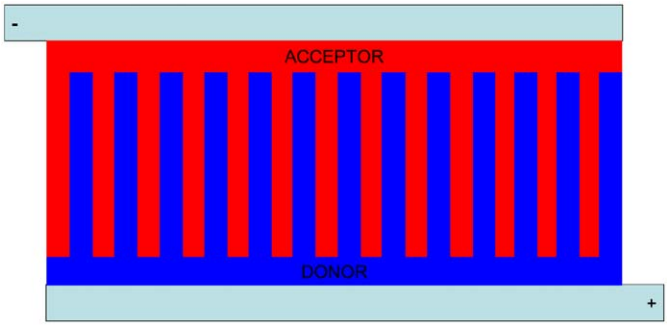

Fig. 9. An ideal structure of donor/acceptor bulk heterojunction polymer solar cells [12].

best entirely solution processed tandem devices was reported by Kin et al. [55]. The key for fabrication of tandem cells is to optimize the interlayer. One type of interlayer was an interface of p-type material and n-type material, such as ZnO/PEDOT [72] and $SnCl_2Pc/F_{16}CuPc$ [73]. Using $SnCl_2Pc/F_{16}CuPc$ as the recombination unit, over 60% increase in PCE was observed. It was found that the tunneling took place at the $SnCl_2Pc/F_{16}CuPc$ interface, providing an effective combination center for electrons and holes. The tunnel junctions by doping had been widely applied in inorganic tandem cells because their low resistance [74]. Au [75], Ag [76], multiple layers like LiF/Al/Au/PEDOT:PSS [77], ITO/PEDOT:PSS [78], Al/MoO_3 [79] and TiO_x/PEDOT:PSS [55] were used as the interlayer for realization tandem solar cells. The operational mechanisms of these different interlayers have not been fully understood yet.

In order to achieve *PCE* of 15%, the best approach is probably through optimization of tandem solar cells. In addition to make functionalized interlayer, the match of electron donors and acceptors with complementary absorption spectra, bandgaps and EQE should be taken into account [80]. A few excellent reviews are carried out on the device physics and the develop-

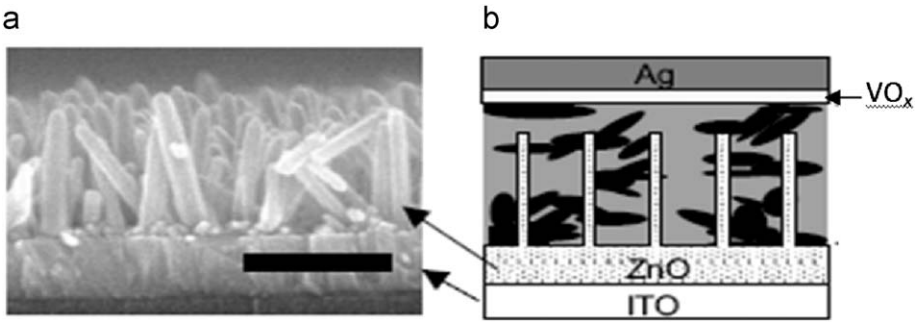

Fig. 10. (a) FE-SEM cross-section image of the ZnO nanorod arrays (scale bar: 300 nm), (b) schematic structure of a ZnO/organic hybrid device with a VO_x buffer layer [15].

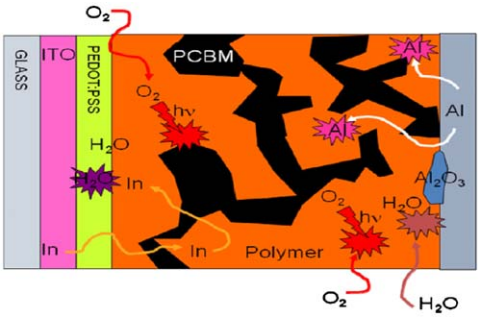

Fig. 11. A graphical overview of the field of stability and degradation of polymer solar cells. [128].

ment situation of organic tandem solar cells [81–83]. Tvingstedt with colleagues have present an interesting device architecture. Two spectrally different cells face to each other under a certain fold angle. Incident light is trapped and the absorption spectrum of the whole cells is broadened. The *PCE* is enhanced by a factor of 1.8 ± 0.3 [84].

4.2. Improving open circuit voltage

The value of V_{OC} is limited primarily by the subtraction of LUMO of the electron acceptor and HOMO of the electron donor as described above. Simultaneously it is also influenced by the contacts between active layer with the electrodes and the morphology of active layer. Table 3a and b summarized the performance of polymer solar cells with buffer layers.

PEDOT:PSS was one of most frequently used buffer layers. PEDOT:PSS was conversional studied in polymer light-emitting diodes (PLEDs). For polymer solar cells, research focuses was on improvement of electrical conductivity of PEDOT:PSS. It was found that the conductivity, morphology and work function of PEDOT:PSS were influenced by post-deposition treatment [98]. The high temperature treatment of PEDOT:PSS can change the paracrystalline structure which was consistent with the molecular lamellae of PEDOT and PSS [99]. The injection efficiency for macroscopic contacts to PEDOT:PSS surfaces can be improved by controlling lamellar orientation at the polymer–metal interface. Doping PEDOT:PSS with different components, such as sorbitol, glycerol [98], mannitol [100] can control the conductive and the work function of PEDOT:PSS. It was also found that the conformational of PEDOT chains in the film changed when ethylene glycol, meso-erythritol and 2-nitroenthanol were doped into PEDOT:PSS. As a result, the conductivity of PEDOT:PSS was enhanced [101]. On doping glycerol into PEDOT:PSS, up to hundred times enhancement in conductivity and lower work function was observed as compared with the un-doped films [98].

LiF was another most frequently used buffer layers. However, the operational mechanism of LiF was still in debate. Forming a tunneling junction [102] to increase built-in potential, an interfacial dipole layer (a few nanometers) to shift the work functions of the electrode [86,103] and dissociated LiF (sub-nanometer) doped into organic semiconductor [104] were proposed operational mechanisms.

Using a thin pentacene interlayer ($\sim$10 nm) in the device of P3HT:PCBM, Kim et al. [89] found that the V_{OC} was increased to 0.73 V. The best performance was observed from the device with 1 nm thickness interlayer instead of 10 nm, but 0.73 V is a large open circuit voltage observed from P3HT:PCBM solar cells.

In conclusion, a few nanometers thick buffer layer not only enlarges the V_{OC} but also acts as a block layer to prevent the reaction between the electrodes with active layer [105,106]. However, the functionality of the buffer layers varies with different materials.

4.3. Towards a controllable morphology

As described in above, the charge transport efficiency η_{tr} is greatly affected by the morphology of the photoactive layer. Proper morphology provides not only an enough interfaces with high separate force for exciton dissociation, but also continuity and correct interpenetrating networks for effective electrons and holes transporting. The precondition for getting optimized morphology is the good miscibility of two materials, which is the inherent character of the material and also dependent on the solvent.

The morphology of polymer-fullerene has been investigated for a long time. Many review articles have made a clear introduction of morphology formation and evolution [107–110]. Janssen et al. has pointed out that both improved crystalline nature of films and increased but controlled demixing between the two constituents therein after annealing is the reason for the increase of the PCE observed in P3HT:PCBM devices [109].

A widely used method to control morphology is to add processing additives [49,52]. Lee et al. [111] suggested that there are two criteria for processing additives: (i) selective solubility of the fullerene component and (ii) higher boiling point than the host solvent. Using these criteria, a better interpenetrating network can be obtained. Fig. 7 shows a schematic depiction of the role of the processing additive in the self-assembly of bulk heterojunction blend materials. In their paper, they argued that three separate phases are formed during the process of liquid–liquid phase separation and drying: a fullerene-alkanedithiol phase, a polymer aggregate phase and a polymer-fullerene phase. The additive with higher boiling point than the chlorobenzene host solvent will remain the PCBM in the solution longer than the semiconducting polymer. Therefore enable the control of the phase separation.

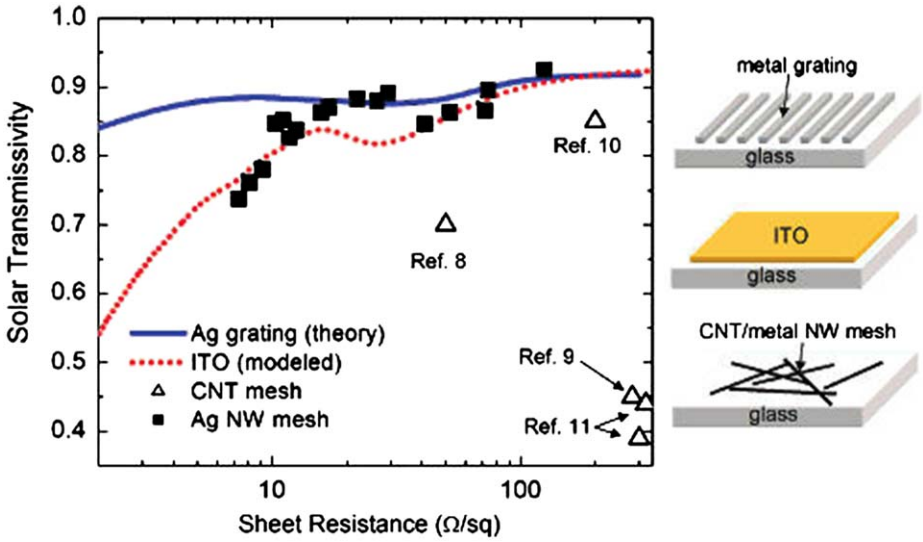

Fig. 12. The conductivity of CNT blended with additional additives [143].

In P3HT:PCBM system, a proposed model for the spin-coating processes was shown in Fig. 8. In this model, Yang with his colleagues [112] have suggested: firstly, the compounds must have lower vapor pressure than that of the primary solvent at room temperature corresponding to a higher boiling point; secondly, the compound must have lower solubility of PCBM than the solvent; thirdly, the compound must be miscible with solvent. All these points were controversial with Lee's findings.

4.4. New device structures

It has been proven that acidic PEDOT:PSS layer was detrimental to active polymer layer, and the low work function metal cathode was easily to be oxidized in air even with a delicate encapsulation. Polymer solar cells with an inverted structure were discovered to overcome above shortages. Table 4 summarized the performance of polymer solar cells with an inverted structure. By using low temperature annealed interfacial buffer layer, cesium carbonate, at top of ITO, Liao and his colleagues have achieved 4.2% of *PCE* from P3HT: PCBM solar cells [113]. However, the PCEs from most of P3HT:PCBM solar cells with an inverted structure, as shown in Table 4, were ~50% of the values (~5% of *PCE*) from P3HT:PCBM solar cells with a normal structure [14,46,49].

In order to optimize the performance of polymer solar cells, an ideal device structure based on bulk heterojunction polymer solar cells was proposed [12]. The ideal micro scale structure for polymer solar cell was shown in Fig. 9. In this structure, nanostructured n-type and p-type phases with a space close to the exciton diffusion length (5–20 nm) would facilitate an efficient separation of charges. The interdigitated and percolated "highways" can ensure unhindered charge carrier transport to the electrodes. However, such well-organized nanostructure is not easy to obtain in classical polymer mixture due to the disorder nature of polymers. Günes has summarized the strategies commonly used today for realizing this structure [6].

Takanezawa et al. [15] reported an inverted cell structure by introducing a ZnO nanorods layer between ITO electrode and active layer. The schematic device structure and a cross-section image of the ZnO nanorod arrays are displayed in Fig. 10. It was found that *FF* was remarkably improved from 50% to 65%, along with a small change in J_{SC} and V_{OC}. The ZnO nanorods work as the electron collectors by shortening the average electron diffusion distance in the PCBM network in the bulk heterojunction. The ZnO nanorods also work as direct paths to transport charge carrier to the ITO electrode, resulting in a decreased charge recombination. Therefore, a larger *FF* was observed.

Substitution of magnesium into a zinc oxide acceptor ($Zn_{1-x}Mg_xO$) results in a simple method to systematically tune the band offset in a p-conjugated polymer–metal oxide hybrid donor–acceptor system in order to maximize the V_{OC}. Olson and colleagues [122] have found that the V_{OC} was increased from 500 mV at x=0 up to values in excess of 900 mV at x=0.35. Their work provided a tool to understand the role of the donor–acceptor band offset in hybrid photovoltaics.

The performance of this nanorod arrays (or called porous structure) is limited by the poor infiltration of polymer into pores of metal oxide with controllable nanostructured dimensions [123,124]. The process of polymer has significantly influence in the infiltration condition. Using dicholorobenzene instead of chloroform will result in an enhanced infiltration which increases the pore size and the vertical order allowing the polymer have enlarged embedded space, improving fill factor [125]. The morphology of ZnO nanostructures in the nanocomposite has direct impacts on the device performance. It was reported that an increased open circuit voltage with a sacrificed short circuit current was observed from ZnO treated with surfactants. However, there was a little increased on overall device efficiency [126].

4.5. Stability of polymer solar cells

While the PCE of the PVC is being improved step by step, the request from commercialization of organic photovoltaic cells (OPVs) has forced the scientists to address the stability of OPVs. Same as other organic devices, the OPVs without encapsulation have very short lifetime, ranging from a few minutes to a few days [127].

The mechanism of the degradation of OPVs through difference pathways was investigated by Jørgensen et al. [128]. Fig. 11 shows the degradation processes. The organic materials and metal used as the electrodes react with oxygen and water which are diffused from both electrodes or lateral of the device are believed the major reason causing short lifetime of OPVs.

Using time-of-flight secondary ion mass spectrometry (TOF-SIMS) methodologies, Krebs with colleagues have demonstrated that the oxygen was diffused into the Al electrode through Al grains and microscopic holes on the Al film [129]. Once inside the

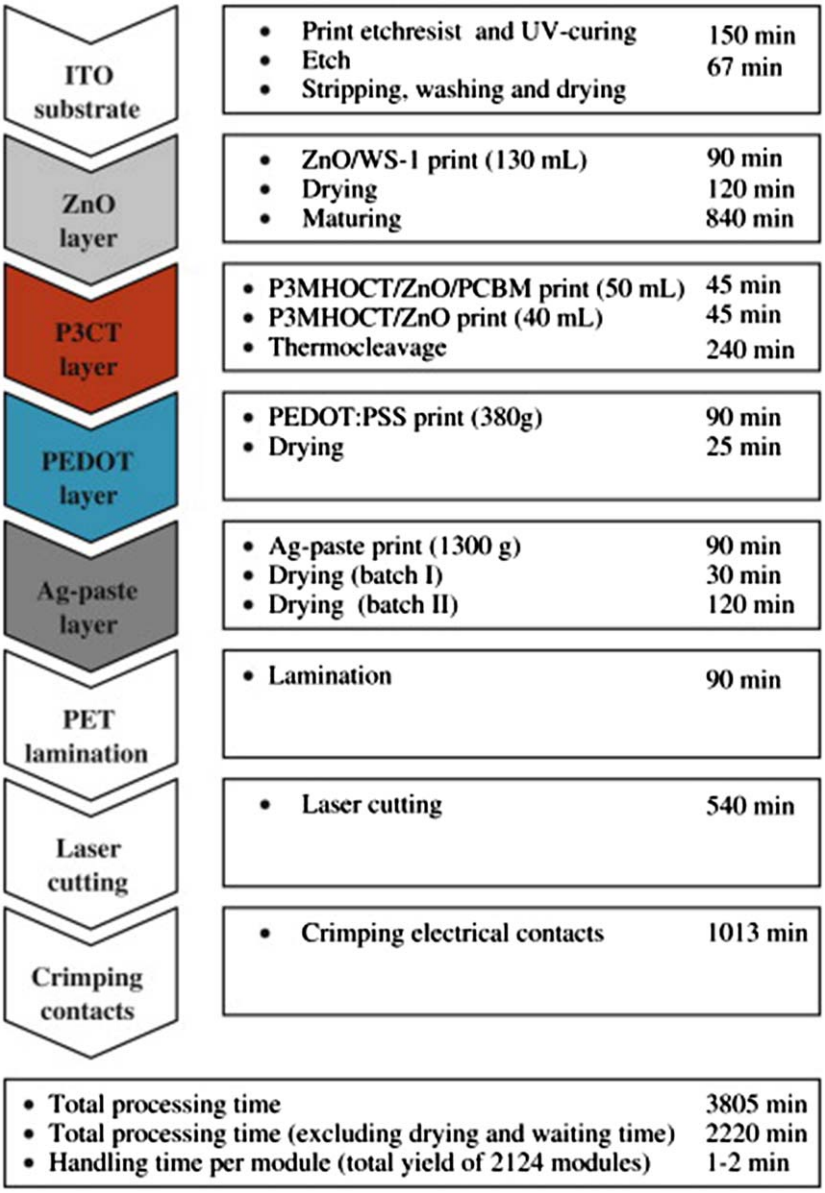

Fig. 13. A process flow chart outlining all the steps along with the process time starting with 200 m of PEDT/ITO substrate that gave a final yield of 2124 completed modules [146].

devices, oxygen was continually diffused in the lateral and vertical plane until reaching the counter electrode. Another prominent degradation pathway was found to be the diffusion of electrode materials into the devices. The degradation is also due to the change of the interface of the devices. Krebs and Norrman [129] observed that indium was diffused in the layer in an OPV with a structure of Al/C60/P3CT/ITO, where P3CT is poly(3-carboxythiophene-co-thiophene). Kawano et al. [130] also found that the resistance of ITO was increased due to the hygroscopic PEDOT:PSS layer absorbed the moisture from the ambient atmosphere.

Thermocleavage materials are used to fabricate air-stable solar cells. The active layer is formed by materials with thermocleavable side chains, the heat treatment converse these soluble materials to insoluble solid films. It was believed that the film formed by these thermocleavable materials is more stable than other common polymers. Krebs et al. has reported a bulk heterojunction polymer solar cells made by thermoleavable materials [131,132]. At first, regiorandom poly-(3-(2-methylhex-2-yl)-oxy-carbonyldithiophene) (P3MHOCT) was blended with PCBM and then spin coated onto top of PEDOT:PSS which was coated on the surface of ITO glass substrates. The thin film layer was then annealed under high temperature up to 250 °C for 10 s. A large area devices device give a *PCE* of 1.5% with a long steady operation time, 500 h [133,134]. They also studied the stability of the devices by tuning different ester groups versus the different eliminated temperature [135].

Hauch with colleagues have investigated the performance of a flexible P3HT:PCBM based modules in outdoor atmosphere. Surprisingly the total efficiency of the modules have not decreased, but increased by 3.3%. This increase was due to a relative increase in *FF* by 10.8%, with a drop in V_{OC} by 6.8%. There is no apparent change in J_{SC} [8].

It was also found that the device with a bulk herterojunction structure is more stable than the device with double layer structure. This is probably due to the fast electron transfer which empties the highly reactive excited state of the polymer [136].

4.6. ITO-free device

ITO is the most popular candidate used for anode to collect generated holes. However, there are many new materials are being developed to replace ITO substrate because of the expensive cost of ITO. The materials are aimed using for future electrode should have high conductivity, high transparency and good mechanical stability on flexible substrates. One of the prominent organic material is PEDOT:PSS. Researchers have made many modifications to improve its conductivity. The conductivity up to 1E+3 S/cm has been reported. New formula of PEDOT:PSS have also been developed and investigated [137,138].

Metal grating is another candidate material used for transparent electrodes. Ag gratings as a transparent electrode for PLEDs with a performance comparable to that of ITO have been reported [139]. Single wall carbon nanotubes (SWCNTs) was another candidate. Random mesh networks of SWCNTs deposited from solution were recently used as the transparent electrodes for organic electronic devices [140], but it has a relatively high sheet resistance. Mixing with other materials to improve conductivity of SWCNTs is one of the approaches. For example, SWCNT meshes was mixed with metallic grids to poses the optical absorption from SWCNT and the high conductive from metallic grids. High conductivity PEDOT:PSS blended with a metallic Ag-grid films is an interesting alternative candidate used for organic solar cells [141,142].

Ag nanowires mesh electrodes reported by Peumans with colleagues exhibited semi-transparency and low sheet resistance. The nanowire meshes are compatible with flexible substrates. Organic solar cells with nanowire meshes as the electrode shown a 19% higher photocurrent was reported [143]. Fig. 12 summarized the conductivity of CNT blended with additional additives.

Using inversion of the layer sequence avoiding to use of ITO without loss of the device performance has been achieved [144]. Alternatively, polymer solar cells based on biodegradable platform was discussed and found to potentially solve the issues related to disposal in the environment in a manner that conventional technologies such as batteries have never achieved [145].

4.7. Manufacturing processes

Polymer solar cells could in principle offer production in high volume at low process cost. Research on the subject has focused mainly on improving the power conversion efficiency for small laboratory cells through optimization of materials and the protocol used for preparation. It is equally important to attempt large-scale production to affirm the likely benefits the technology may have to offer in terms of processing ease and cost. Krebs with colleagues [146–151] overviewed the possibility of manufacturing processing organic solar cells. Other scientists and engineers also addressed this topic [152–157].

Fig. 13 shows a typical process flow chart outlining all the steps along with the process time starting with 200 m of PEDO T/ITO substrate that gave a final yield of 2124 completed modules. The critical process was to print PEDOT:PSS on top of polymer layer.

Various methods have been demonstrated to manufacture large OPV modules and a lifetime of 5000 h from OPV modules was reported. With optimized materials synthesis, photoactive layer ink formulation, and module design and fabrication, long lifetime with high power conversion efficiency OPV solar cells is anticipated to be demonstrated. However, OPV solar cells are not generally produced commercially today. One exception is the company Konarka Technologies which in 2008 opened a factory with the capacity to produce a gigawatt's worth of polymer-fullerene solar cells each year. The initial cells from the factory are 3–5% efficient, and only last a couple years, but the company has stated that it would eventually be able to improve both the efficiency and durability. The company expects to initially sell the cells in for number of niche applications: For example, in laptop-recharging briefcases, put into tents, umbrellas, awnings and as window tinting (since the cells can be made transparent).

5. Conclusion and outlook

Donor–acceptor bulk heterojunction polymer solar cells are currently showing power convention efficiency of more than 6%. Thermal annealing, slow drying, additive processing, controllable self-assembly morphology, adding buffer layer and new device structure can play an important role in achieving high power convention efficiency. In order to obtain more than 10% of power convention efficiency from single layer polymer solar cells, more investigation must be carried out to explore the fundamental mechanisms and develop new materials. Development of new materials is an urgent issue. Many scientists believe there is a best way to get more absorption and higher open circuit voltage, and a better charge transfer condition. Toward a controllable interpenetrating network in the films is also important for optimization of solar cell performance. In addition, designing novel structures to gain more absorption and controllable local order of materials are possible approaches to realize high efficiency and high stability of polymer solar cells.

Acknowledgement

The author X. Gong would like to thank the Joint Research Fund for Overseas Chinese Scholars, the National Science Foundation of China (#50828301). The authors W. Z. Cai and Y. Cao would like to thank NSFC (#50990065) and MOST (#2009CB603601).

References

[1] C.J. Brabec, Organic photovoltaics: technology and market, Sol. Energy Mater. Sol. Cells 83 (2004) 273–292.
[2] F.C. Krebs, Fabrication and processing of polymer solar cells: a review of printing and coating techniques, Sol. Energy Mater. Sol. Cells 93 (2009) 394–412.
[3] R. Gaudiana, C.J. Brabec, Organic materials—fantastic plastic, Nat. Photonics 2 (2008) 287–289.
[4] S.H. Park, A. Roy, S. Beaupré, S. Cho, N. Coates, J.S. Moon, D. Moses, M. Leclerc, K. Lee, A.J. Heeger, Bulk heterojunction solar cells with internal quantum efficiency approaching 100%, Nat. Photonics 3 (2009) 297–303.
[5] Y.Y. Liang, D.Q. Feng, Y. Wu, S.T. Tsai, G. Li, Gang, C. Ray, L.P. Yu, Highly efficient solar cell polymers developed via fine-tuning of structural and electronic properties, J. Am. Chem. Soc. 131 (2009) 7792–7799.
[6] S. Günes, H. Neugebauer, N.S. Sariciftci, Conjugated polymer-based organic solar cells, Chem. Rev. 107 (2007) 1324–1338.
[7] E.A. Katz, S. Gevorgyan1, M.S. Orynbayev, F.C. Krebs, Out-door testing and long-term stability of plastic solar cells, Eur. Phys. J. Appl. Phys. 36 (2007) 307–311.
[8] J.A. Hauch, P. Schilinsky, S.A. Choulis, R. Childers, M. Biele, C.J. Brabec, Flexible organic P3HT:PCBM bulk-heterojunction modules with more than 1 year outdoor lifetime, Sol. Energy Mater. Sol. Cells 92 (2008) 727–731.
[9] A.J. Heeger, Nobel lecture: semiconducting and metallic polymers: the fourth generation of polymeric materials, Rev. Mod. Phys. 73 (2001) 681–700.
[10] S. Barth, H. Bässler, Intrinsic photoconduction in PPV-type conjugated polymers, Phys. Rev. Lett. 79 (1997) 4445–4448.
[11] T. Ameri, G. Dennler, C. Waldauf, P. Denk, K. Forberich, M.C. Scharber, C.J. Brabec, K. Hingerl, Realization, characterization, and optical modeling of inverted bulk-heterojunction organic solar cells, J. Appl. Phys. 103 (2008) 084506-1-6.
[12] H. Hoppe, N.S. Sariciftci, Polymer solar cells, Adv. Polym. Sci. 214 (2008) 1–86.
[13] Y. Liang, Y. Wu, D. Feng, S.T. Tsai, H.J. Son, G. Li, L. Yu, Development of new semiconducting polymers for high performance solar cells, J. Am. Chem. Soc. 131 (2009) 56–57.

[14] J.Y. Kim, S.H. Kim, H. Lee, K. Lee, W. Ma, X. Gong, A.J. Heeger, New architecture for high-efficiency polymer photovoltaic cells using solution - based titanium oxide as an optical spacer, Adv. Mater. 18 (2006) 572–576.
[15] K. Takanezawa, K. Tajima, K. Hashimoto, Efficiency enhancement of polymer photovoltaic devices hybridized with ZnO nanorod arrays by the introduction of a vanadium oxide buffer layer, Appl. Phys. Lett. 93 (2008) 063308-1-3.
[16] C.J. Brabec, G. Zerza, G. Cerullo, S.D. Silvestri, S. Luzzati, J.C. Hummelen, S. Sariciftci, Tracing photoinduced electron transfer process in conjugated polymer/fullerene bulk heterojunctions in real time, Chem. Phys. Lett. 340 (2001) 232–236.
[17] V.D. Mihailetchi, J. Wildeman, P.W.M. Blom, Space–charge limited photocurrent, Phys. Rev. Lett. 94 (2005) 126602-1-4.
[18] V.D. Mihailetchi, P.W.M. Blom, J.C. Hummelen, M.T. Rispens, Cathode dependence of the open-circuit voltage of polymer: fullerene bulk heterojunction solar cells, J. Appl. Phys. 94 (2003) 6849–6854.
[19] V.D. Mihailetchi, L.J.A. Koster, P.W.M. Blom, Effect of metal electrodes o the performance of polymer: fullerene bulk heterojunction solar cells, Appl. Phys. Lett. 85 (2004) 970–972.
[20] C.J. Brabec, A. Cravino, D. Meissner, N.S. Sariciftci, T. Fromherz, M.T. Rispens, L. Sanchez, J.C. Hummelen, Origin of the open circuit voltage of plastic solar cells, Adv. Funct. Mater. 11 (2001) 374–380.
[21] M.C. Scharber, D. Mühlbacher, M. Koppe, P. Denk, C. Waldauf, A.J. Heeger, C.J. Brabec, Design rules for donors in bulk-heterojunction solar cells—towards 10% energy-conversion efficiency, Adv. Mater. 18 (2006) 789–794.
[22] Q.M. Zhou, Q. Hou, L. Zheng, X. Deng, D. Yu, Y. Cao, Fluorene-based low band-gap copolymers for high performance photovoltaic devices, Appl. Phys. Lett. 84 (2004) 1653–1655.
[23] N. Blouin, A. Michaud, M. Leclerc, A low-bandgap poly(2, 7-carbazole) derivatives for use in high-performance solar cells, Adv. Mater. 19 (2007) 2295–2300.
[24] C.J. Brabec, J.R. Durrant, Solution-processed organic solar cells, MRS Bull. 33 (2008) 670–675.
[25] B.C. Thompson, J.M. Frechet, Polymer-fullerene composite solar cells, Angew. Chem. Int. Ed. 47 (2008) 58–77.
[26] X. Gong, M.H. Tong, Y.J. Xia, W.Z. Cai, J.S. Moon, Y. Cao, G. Yu, C.L. Shieh, B. Nilsson, A.J. Heeger, High-detectivity polymer photodetectors with spectral response from 300 nm to 1450 nm, Science 325 (2009) 1665–1667.
[27] F. Banishoeib, A. Henckens, S. Fourier, G. Vanhooyland, M. Breselge, J. Manca, T.J. Cleij, L. Lutsen, D. Vanderzande, L.H. Nguyen, H. Neugebauer, N.S. Sariciftci, Synthesis of poly(2,5-Thienylene Vinylene) and its derivatives: low band gap materials for photovoltaics, Thin Solid Films 516 (2008) 3978–3988.
[28] F. Banishoeib, P. Adriaensens, S. Berson, S. Guillerez, O. Douheret, J. Manca, S. Fourier, T.J. Cleij, L. Lutsen, D. Vanderzande, The synthesis of regio-regular poly(3-alkyl-2,5-thienylene vinylene) derivatives using lithium bis(trimethylsilyl)amide (LHMDS) in the dithiocarbamate precursor route, Sol. Energy Mater. Sol. Cells 91 (2007) 1026–1034.
[29] C.Y. Yu, C.P. Chen, S.H. Chan, G.W. Hwang, C. Ting, Thiophene/phenylene/thiophene-based low-bandgap conjugated polymers for efficient near-infrared photovoltaic applications, Chem. Mater. 21 (2009) 3262–3269.
[30] W. Yue, Y. Zhao, S.Y. Tian, Z.Y. Xie, Y.H. Geng, F.S. Wang, Novel NIR-absorbing conjugated polymers for efficient polymer solar cells: effect of alkyl chain length on device performance, J. Mater. Chem. 19 (2009) 2199–2206.
[31] T.B. Singh, N. Marjanovic, G.J. Matt, S. Günes, N.S. Sariciftci, A.M. Ramil, A. Andreev, H. Sitter, R. Schwödiauer, S. Bauer, High-mobility n-channel organic field-effect transistors based on epitaxially grown C_{60} films, Org. Electron. 6 (2005) 1199–1566.
[32] M. Campoy-Quiles, T. Ferenczi, T. Agostinelli, P.G. Etchegoin, Y. Kim, T.D. Anthopoulos, P.N. Stavrinou, D.D.C. Bradley, J. Nelson, Morphology evolution via self-organization and lateral and vertical diffusion in polymer: fullerene solar cell blends, Nat. Mater. 7 (2008) 158–164.
[33] M. Reyes-Reye, K. Kim, D.L. Carroll, High-efficiency photovoltaic devices based on annealed poly (3-hexylthiophene) and 1-(3-methoxycarbonyl)-propyl-1-phenyl-(6, 6)C-61 blends, Appl. Phys. Lett. 87 (2005) 083506-1-3.
[34] M.Y. Chiu, U.S. Jeng, C.H. Su, K.S. Liang, K.H. Wer, Simultaneous use of small- and wide-angle X-ray techniques to analyze nanometerscale phase separation in polymer heterojunction solar cells, Adv. Mater. 20 (2008) 2573–2578.
[35] T. Erb, U. Zhokhavets, G. Gobsch, S. Raleva, B. Stühn, P. Schilinsky, C. Waldauf, C.J. Brabec, Correlation between structural and optical properties of composite polymer/fullerene films for organic solar cells, Adv. Func. Mater. 15 (2005) 1193–1196.
[36] C.Y. Yang, J. Hu, A.J. Heeger, Molecular structure and dynamics at the interfaces within bulk heterojunction materials for solar cells, J. Am. Chem. Soc. 128 (2006) 12007–12013.
[37] V.D. Mihailetchi, H. Xie, B.D. Boer, L.J.A. Koster, P.W.M. Blom, Charge transport and photocurrent generation in poly (3-hexylthiophene): methanofullerene bulk-heterojunction solar cells, Adv. Funct. Mater. 16 (2006) 699–708.
[38] J. Huang, G. Li, Y. Yang, Influence of composition and heat-treatment on the charge transport properties of poly (3-hexylthiophene) and [6,6]-phenyl C/sub 61/-butyric acid methyl ester blends, Appl. Phys. Lett. 87 (2005) 112105-1-3.
[39] T.J. Savenije, J.E. Kroeze, X. Yang, J. Loos, The effect of thermal treatment on the morphology and charge carrier dynamics in a polythiophene-fullerene bulk heterojunction, Adv. Funct. Mater. 15 (2005) 1260–1266.
[40] C. Müller, T.A.M. Ferenczi, M. Campoy-Quiles, J.M. Frost, D.D.C. Bradley, P. Smith, N. Stingelin-Stutzmann, J. Nelson, Binary organic photovoltaic blends: a simple rationale for optimum compositions, Adv. Mater. 20 (2008) 3510–3515.
[41] T.M. Clarke, A.M. Ballantyne, J. Nelson, D.D.C. Bradley, J.R. Durrant, Free energy control of charge photogeneration in polythiophene/fullerene solar cells: the influence of thermal annealing on P3HT/PCBM blends, Adv. Funct. Mater. 18 (2008) 4029–4035.
[42] I.W. Hwang, D. Moses, A.J. Heeger, Photoinduced carrier generation in P3HT/PCBM bulk heterojunction materials, J. Phys. Chem. C 112 (2008) 4350–4354.
[43] R.C. Hioms, R. Bettignies, J. Leroy, S. Bailly, M. Firon, C. Sentein, A. Khoukh, H. Preud'homme, C. Dagron-Lartigau, High molecular weights, polydispersities, and annealing temperatures in the optimization of bulk-heterojunction photovoltaic cells based on poly(3-hexylthiophene) or poly(3-butylthiophene), Adv. Funct. Mater. 16 (2006) 2263–2273.
[44] Y. Kim, S. Cook, S.M. Tuladhar, S.A. Choulis, J. Nelson, J.R. Durrant, D.D.C. Bradley, M. Giles, I. Mcculloch, C. Ha, M. Ree, A strong regioregularity effect in self-organizing conjugated polymer films and high-efficiency polythiophene: fullerene solar cells, Nat. Mater. 5 (2006) 197–203.
[45] A.J. Moulé, K. Meerholz, Controlling morphology in polymer-fullerene mixtures, Adv. Mater. 20 (2008) 240–245.
[46] F. Padinger, R.S. Rittberger, N.S. Sariciftci, Effects of postproduction treatment on plastic solar cells, Adv. Funct. Mater. 13 (2003) 85–88.
[47] M. Al-Ibrahim, O. Ambacher, S. Sensfuss, G. Gobsch, Effects of solvent and annealing on the improved performance of solar cells based on poly (3-hexylthiophene): fullerene, Appl. Phys. Lett. 86 (2005) 201120-1-3.
[48] Y. Zhao, Z. Xie, Y. Qu, Y. Geng, L. Wang, Solvent-vapor treatment induced performance enhancement of poly (3-hexylthiophene): methanofullerene bulk-heterojunction photovoltaic cells, Appl. Phys. Lett. 90 (2007) 43504-1-3.
[49] W. Wang, H. Wu, C. Yang, C. Luo, Y. Zhang, J. Chen, Y. Cao, High-efficiency polymer photovoltaic devices from regioregular poly (3-hexylthiophene-2,5-diyl) and [6,6]-phenyl-C_{61}-butyric acid methl ester processed with oleic acid surfactant, Appl. Phys. Lett. 90 (2007) 183512-1-3.
[50] G. Dennler, M.C. Scharber, C.J. Brabec, Polymer-fullerene bulk-heterojunction solar cells, Adv. Mater. 21 (2009) 1–16.
[51] E. Wang, L. Wang, L. Lan, C. Luo, W. Zhuang, J. Peng, Y. Cao, High-performance polymer heterojunction solar cells of a polysilafluorene derivative, Appl. Phys. Lett. 92 (2008) 033307-1-3.
[52] J. Peet, J.Y. Kim, N.E. Coates, W.L. Ma, D. Moses, A.J. Heeger, G.C. Bazan, Efficiency enhancement in low-bandgap polymer solar cells by processing with alkane dithiols, Nat. Mater. 6 (2007) 497–500.
[53] I. Gur, N.A. Fromer, C. Chen, A.G. Kanaras, A.P. Alivisatos, Hybrid solar cells with prescribed nanoscale morphologies based on hyperbranched semiconductor nanocrystals, Nano Lett. 7 (2007) 409–414.
[54] B. Sun, H.J. Snaith, A.S. Dhoot, S. Westenhoff, N.C. Greenham, Vertically segregated hybrid blends for photovoltaic devices with improved efficiency, J. Appl. Phys. 97 (2005) 14914-1-6.
[55] J.Y. Kim, K. Lee, N.E. Coates, D. Moses, T. Nguyen, M. Dante, A.J. Heeger, Efficient tandem polymer solar cells fabricated by all-solution processing, Science 317 (2007) 222–225.
[56] C. Winder, N.S. Sariciftci, Low bandgap polymers for photon harvesting in bulk heterojunction solar cells, J. Mater. Chem. 14 (2004) 1077–1086.
[57] J.W. Chen, Y. Cao, Development of novel conjugated donor polymers for high-efficiency bulk-heterojunction photovoltaic devices, Acc. Chem. Res. (2009).
[58] E. Bundgaard, F.C. Krebs, Low band gap polymers for organic photovoltaics, Sol. Energy Mater. Sol. Cells 91 (2007) 954–985.
[59] M.M. Wienk, J.M. Kroon, W.J.H. Verhees, J. Knol, J.C. Hummelen, P.A. van Hal, R.A.J. Janssen, Efficient methano [70] fullerene/MDMO-PPV bulk heterojunction photovoltaic cells, Angew. Chem. 115 (2003) 3371–3375.
[60] F.B. Kooistra, V.D. Mihailetchi, L.M. Popescu, D. Kronholm, P.M. Blom, J.C. Hummelen, New C-84 derivative and its application in a bulk heterojunction solar cell, Chem. Mater. 18 (2006) 3068–3073.
[61] R.B. Ross, C.M. Cardona, D.M. Guldi, S.G. Sankaranarayanan, M.O. Reese, N. Kopidakis, J. Peet, B. Walker, G.C. Bazan, E.V. Keuren, B.C. Holloway, M. Drees, Endohedral fullerenes for organic photovoltaic devices, Nat. Mater. 8 (2009) 208–212.
[62] F.G. Brunetti, X. Gong, M. Tong, A.J. Heeger, F. Wudl, Angew. Chem., in press.
[63] X. Gong, M.H. Tong, F.G. Brunetti, D. Moses, F. Wudl, A.J. Heeger, JACS, submitted for publication.
[64] B.R. Saunders, M.L. Turner, Nanoparticle-polymer photovoltaic cells, Adv. Colloid Interface 138 (2008) 1–23.
[65] W.J.E. Beek, M.M. Wienk, M. Kemerink, X.N. Yang, R.A.J. Janssen, Hybrid zinc oxide conjugated polymer bulk heterojunction solar cells, J. Phys. Chem. B 109 (2005) 9505–9516.
[66] K. Lee, J.Y. Kim, S.H. Park, S.H. Kim, S. Cho, A.J. Heeger, Air-stable polymer electronic devices, Adv. Mater. 19 (2007) 2445–2449.
[67] J.K. Lee, N.E. Coates, S. Cho, N.S. Cho, D. Moses, G.C. Bazan, K. Lee, A.J. Heeger, Efficacy of TiO_x optical spacer in bulk-heterojunction solar cells processed with 1,8-octanedithiol, Appl. Phys. Lett. 92 (2008) 243308-1-3.

[68] C. Zhang, S.W. Tong, C. Jiang, E.T. Kang, D.S .H. Chan, C. Zhu, Efficient multilayer organic solar cells using the optical interference peak, Appl. Phys. Lett. 93 (2008) 043307-1-3.
[69] P. Würfel, in: Physics of Solar Cells, Wiley-VCH, Berlin, Germany, 2004.
[70] J. Drechsel, B. Mannig, F. Kozlowski, D. Gebeyehu, A. Werner, M. Koch, K. Leo, M. Pfeiffer, High efficiency organic solar cells based on single or multiple PIN structures, Thin Solid Films 451-452 (2004) 515–517.
[71] O. Hagemann, M. Bjerring, N.C. Nielsen, F.C. Krebs, All solution processed tandem polymer solar cells based on thermocleavable materials, Sol. Energy Mater. Sol. Cells 92 (2008) 1327–1335.
[72] J. Gilot, M.M. Wienk, R.A.J. Janssen, Double and triple junction polymer solar cells processed from solution, Appl. Phys. Lett. 90 (2007) 143512-1-3.
[73] B. Yu, F. Zhu, H. Wang, G. Li, D. Yan, All-organic tunnel junctions as connecting units in tandem organic solar cell, J. Appl. Phys. 104 (2008) 114503-1-5.
[74] D.L. Miller, S.W. Zehr, J.J.S. Harris, GaAs–AlGaAs tunnel junctions for multigap cascade solar cells, J. Appl. Phys 53 (1982) 744–748.
[75] J. Drechsel, B. Männig, F. Kozlowski, M. Pfeiffer, K. Leo, H. Hoppe, Efficient organic solar cells based on a double p-i-n architecture using doped wide-gap transport layers, Appl. Phys. Lett. 86 (2005) 244102-1-3.
[76] A. Yakimov, S.R. Forrest, High photovoltage multiple-heterojunction organic solar cells incorporating interfacial metallic nanoclusters, Appl. Phys. Lett 80 (2002) 1667–1669.
[77] A. Hadipour, B. de Boer, J. Wildeman, F.B. Kooistra, J.C. Hummelen, M.G.R. Turbiez, M.M. Wienk, R.A. Janssen, P.W.M. Blom, Solution-Processed organic tandem solar cells, Adv. Funct. Mater. 16 (2006) 1897–1903.
[78] K. Kawano, N. Lto, T. Nishimori, J. Sakai, Open circuit voltage of stacked bulk heterojunction organic solar cells, Appl. Phys. Lett. 88 (2006) 073514-1-3.
[79] D.W. Zhao, X.W. Sun, C.Y. Jiang, A.K.K. Kyaw, G.Q. Lo, D.L. Kwong, Efficient tandem organic solar cells with an Al/MoO_3 intermediate layer, Appl. Phys. Lett. 93 (2008) 083305-1-3.
[80] G. Dennler, M.C. Scharber, T. Ameri, P. Denk, K. Forberich, C. Waldauf, C.J. Brabec, Design rules for donors in bulk-heterojunction tandem solar cells—towards 15% energy-conversion efficiency, Adv. Mater. 20 (2008) 579–583.
[81] A. Hadipour, B. de Boer, P.W.M. Blom, Organic tandem and multi-junction solar cells, Adv. Funct. Mater. 18 (2008) 169–181.
[82] T. Ameri, G. Dennler, C. Lungenschmied, C.J. Brabec, Organic tandem solar cells: a review, Energy Environ. Sci. 2 (2009) 347–363.
[83] A. Hadipour, B. de Boer, P.W.M. Blom, Device operation of organic tandem solar cells, Org. Electron. 9 (2008) 617–624.
[84] K. Tvingstedt, V. Andersson, F.L. Zhang, O. Inganäs, Folded reflective tandem polymer solar cell doubles efficiency, Appl. Phys. Lett. 91 (2007) 123514-1-3.
[85] F.S. Wen, W.L. Li, H.Z. Wei, Effect of electrode modification on organic photovoltaic devices, Mater. Chem. Phys. 95 (2006) 94–98.
[86] C.J. Brabec, S.E. Shaheen, C. Winder, N.S. Sariciftci, P. Denk, Effect of LiF/metal electrodes on the performance of plastic solar cells, Appl. Phys. Lett. 80 (2002) 1288–1290.
[87] Y. Zhao, Z. Xie, Y. Qu, Y. Geng, L. Wang, Effects of thermal annealing on polymer photovoltaic cells with buffer layers and in situ formation of interfacial layer for enhancing power conversion efficiency, Synth. Met. 158 (2008) 908–911.
[88] F.C. Chen, J.L. Wu, S.S. Yang, K.H. Hsieh, W.C. Chen, Cesium carbonate as a functional interlayer for polymer photovoltaic devices, J. Appl. Phys. 103 (2008) 103721-1-5.
[89] J.H. Kim, S.Y. Huh, T. Kim, H. Lee, Thin pentacene interlayer for polymer bulk-heterojunction solar cell, Appl. Phys. Lett. 93 (2008) 143305-1-3.
[90] A. Hayakawa, O. Yoshikawa, K. Fujieda, K. Uehara, S. Yoshikawa, High performance polythiophene/fullerene bulk-heterojunction solar cell with a TiO_x hole blocking layer, Appl. Phys. Lett. 90 (2007) 163517-1-3.
[91] Q.S. Wei, T. Nishizawa, K. Tajima, K. Hashimoto, Self-organized buffer layers in organic solar cells, Adv. Mater. 20 (2008) 2211–2216.
[92] M.Y. Chang, C.S. Wu, Y.F. Chen, B.Z. Hsieh, W.Y. Huang, K.S. Ho, T.H. Hsieh, Y.K. Han, Polymer solar cells incorporating one-dimensional polyaniline nanotubes, Org. Electron. 9 (2008) 1136–1139.
[93] A.W. Hains, T.J. Marks, High-efficiency hole extraction/electron-blocking layer to replace poly(3, 4-ethylenedioxythiophene):poly(styrene sulfonate) in bulk-heterojunction polymer solar cells, Appl. Phys. Lett. 92 (2008) 023504-1-3.
[94] S.W. Tong, C.F. Zhang, C.Y. Jiang, G. Liu, Q.D. Ling, E.T. Kang, D.S.H. Chan, C. Zhu, Improvement in the hole collection of polymer solar cells by utilizing gold nanoparticle buffer layer, Chem. Phys. Lett. 453 (2008) 73–76.
[95] V. Shrotriya, G. Li, Y. Yao, C.W. Chu, Y. Yang, Transition metal oxides as the buffer layer for polymer photovoltaic cells, Appl. Phys. Lett. 88 (2006) 073508-1-3.
[96] W.J. Yoon, P.R. Berger, 4.8% efficient poly(3-hexylthiophene)-fullerene derivative (1: 0.8) bulk heterojunction photovoltaic devices with plasma treated AgO_x/indium tin oxide anode modification, Appl. Phys. Lett. 92 (2008) 013306.
[97] S. Chaudhary, H. Lu, A.M. Müller, C.J. Bardeen, M. Ozkan, Hierarchical placement and associated optoelectronic impact of carbon nanotubes in polymer-fullerene solar cells, Nano Lett. 7 (2007) 1973–1979.
[98] J. Huang, P.F. Miller, J.S. Wilson, A.J. de Mello, J.C. de Mello, D.D.C. Bradley, Investigation of the effects of doping and post-deposition treatments on the conductivity, morphology, and work function of poly(3,4-ethylenedioxythiophene)/poly(styrene sulfonate) films, Adv. Funct. Mater. 15 (2005) 290–296.
[99] C. Ionescu-Zanetti, A. Mechler, S.A. Carter, R. Lal, Semiconductive polymer blends: correlating structure with transport properties at the nanoscale, Adv. Mater. 16 (2004) 385–389.
[100] C.J. Ko, Y.K. Lin, F.C. Chen, C.W. Chu, Modified buffer layers for polymer photovoltaic devices, Appl. Phys. Lett. 90 (2007) 63509-1-3.
[101] J. Ouyang, C.W. Chu, F.C. Chen, Q. Xu, Y. Yang, High-conductivity poly (3,4-ethylene dioxythiophene) : poly(styrene sulfonate) film and its application in polymer optoelectronic devices, Adv. Funct. Mater. 15 (2005) 203–208.
[102] L.S. Hung, C.W. Tang, M.G. Mason, Enhanced electron injection in organic electroluminescence devices using an Al/LiF electrode, Appl. Phys. Lett. 70 (1997) 152–154.
[103] S.E. Shaheen, C.J. Brabec, N.S. Sariciftci, G.E. Jabbour, Effects of inserting highly polar salts between the cathode and active layer of bulk heterojunction photovoltaic devices, Mat. Res. Soc. Symp. Proc. 665 (2001) 219–418.
[104] X.Y. Deng, S.W. Tong, L.S. Hung, Y.Q. Mo, Y. Cao, Role of ultrathin Alq_3 and LiF layers in conjugated polymer light-emitting diodes, Appl. Phys. Lett. 82 (2003) 3104–3106.
[105] W.J.H. Gennip, J.K.J. van Duren, P.C. Thüne, The interfaces of poly(p-phenylene vinylenes) and fullerene derivatives with Al, LiF, and Al/LiF studied by secondary ion mass spectroscopy and x-ray photoelectron spectroscopy: formation of AlF_3 disproved, J. Chem. Phys. 117 (2002) 5031–5035.
[106] H. Gommans, B. Verreet, B.P. Rand, R. Muller, J. Poortmans, P. Heremans, J. Genoe, On the role of bathocuproine in organic photovoltaic cells, Adv. Funct. Mater. 18 (2008) 3686–3691.
[107] B.C. Thompson, J.M.J. Fréchet, Polymer-fullerene composite solar cells, Angew. Chem. Int. Ed. 47 (2008) 58–77.
[108] H. Hoppe, N.S. Sariciftci, Morphology of polymer/fullerene bulk heterojunction solar cells, J. Mater. Chem. 16 (2006) 45–61.
[109] X.N. Yang, J. Loos, S.C. Veenstra, W.J.H. Verhees, M.M. Wienk, J.M. Kroon, M.A.J. Michels, R.A.J. Janssen, Nanoscale morphology of high-performance polymer solar cells, Nano Lett. 5 (2005) 579–583.
[110] X. Yang, J. Loos, Toward high-performance polymer solar cells: the importance of morphology control, Macromolecules 40 (2007) 1353–1362.
[111] J.K. Lee, W.L. Ma, C.J. Brabec, J. Yuen, J.S. Moon, J.Y. Kim, K. Lee, G.C. Bazan, A.J. Heeger, Processing additives for improved efficiency from bulk heterojunction solar cells, J. Am. Chem. Soc. 130 (2008) 3619–3623.
[112] Y. Yao, J. Hou, Z. Xu, G. Li, Y. Yang, Effects of solvent mixtures on the nanoscale phase separation in polymer solar cells, Adv. Funct. Mater. 18 (2008) 1783–1789.
[113] H.H. Liao, L.M. Chen, Z. Xu, G. Li, Y. Yang, Highly efficient inverted polymer solar cell by low temperature annealing of Cs2CO3 interlayer, Appl. Phys. Lett. 92 (2008) 173303-1-3.
[114] B.Y. Yu, A. Tsai, S.P. Tsai, K.T. Wong, Y. Yang, C.W. Chu, J.J. Shyue, Efficient inverted solar cells using TiO_2 nanotube arrays, Nanotechnology 19 (2008) 255202-1-5.
[115] G. Li, C.W. Chu, V. Shrotriya, J. Huang, Y. Yang, Efficient inverted polymer solar cells, Appl. Phys. Lett. 88 (2006) 253503-1-3.
[116] M.S. White, D.C. Olson, S.E. Shaheen, N. Kopidakis, D.S. Ginley, Inverted bulk-heterojunction organic photovoltaic device using a solution-derived ZnO underlayer, Appl. Phys. Lett. 89 (2006) 143517-1-3.
[117] C. Waldauf, M. Morana, P. Denk, P. Schilinsky, K. Coakley, S.A. Choulis, C.J. Brabec, Highly efficient inverted organic photovoltaics using solution based titanium oxide as electron selective contact, Appl. Phys. Lett. 89 (2006) 233517-1-3.
[118] S.K. Hau, H.L. Yip, O. Acton, N.S. Baek, H. Ma, A.K.Y. Jen, Interfacial modification to improve inverted polymer solar cells, J. Mater. Chem. 18 (2008) 5113–5119.
[119] C. Tao, S. Ruan, X. Zhang, G. Xie, L. Shen, X. Kong, W. Dong, C. Liu, W. Chen, Performance improvement of inverted polymer solar cells with different top electrodes by introducing a MoO_3 buffer layer, Appl. Phys. Lett. 93 (2008) 9193307-1-3.
[120] K. Takanezawa, K. Hirota, Q-S Wei, K. Tajima, K. Hashimoto, Efficient charge collection with ZnO nanorod array in hybrid photovoltaic devices, J. Phys. Chem. C 111 (2007) 7218–7223.
[121] S.K. Hau, H.L Yip, N.S. Baek, J. Zhou, K. O'Malley, A.K.Y. Jen, Air-stable inverted flexible polymer solar cells using zinc oxide nanoparticles as an electron selective layer, Appl. Phys. Lett. 92 (2008) 253301-1-3.
[122] D.C. Olson, S.E. Shaheen, M.S. White, W.J. Mitchell, R.T. Collins, D.S. Ginley, et al., Band-offset engineering for enhanced open-circuit voltage in polymer-oxide hybrid solar cells, Adv. Funct. Mater. 17 (2007) 264–269.
[123] D.C. Olson, J. Piris, R.T. Collins, S.E. Shaheen, D.S. Ginley, Hybrid photovoltaic devices of polymer and ZnO nanofiber composites, Thin Solid Films 496 (2006) 26–29.
[124] J. Bouclé, P. Ravirajan, J. Nelson, Hybrid polymer–metal oxide thin films for photovoltaic applications, J. Mater. Chem. 17 (2007) 3141–3153.
[125] D.C. Olson, Y.J. Lee, M.S. White, N. Kopidakis, S.E. Shaheen, D.S. Ginley, J.A. Voigt, J.W.P. Hsu, Effect of polymer processing on the performance of poly(3-hexylthiophene)/ZnO nanorod photovoltaic devices, J. Phys. Chem. C 111 (2007) 16640–16645.
[126] D.C. Olson, S.E. Shaheen, R.T. Collins, D.S. Ginley, The effect of atmosphere and ZnO morphology on the performance of hybrid poly(3-hexylthiophene)/ZnO nanofiber photovoltaic devices, J. Phys. Chem. C 111 (2007) 16670–16678.

[127] F.C. Krebs, H. Spanggaard, Significant improvement of polymer solar cell stability, Chem. Mater. 17 (2005) 5235–5237.
[128] M. Jørgensen, K. Norrman, F.C. Krebs, Stability/degradation of polymer solar cells, Sol. Energy Mater. Sol. Cells 92 (2008) 686–714.
[129] F.C. Krebs, K. Norrman, Analysis of the failure mechanism for a stable organic photovoltaic during 10 000 h of testing, Prog. Photovolt.: Res. Appl. 15 (2007) 697–712.
[130] K. Kawano, R. Pacios, D. Poplavskyy, J. Nelson, D.D.C. Bradley, J.R. Durrant, Degradation of organic solar cells due to air exposure, Sol. Energy Mater. Sol. Cells 90 (2006) 3520–3530.
[131] F.C. Kreb, Y. Thomann, R. Thomann, J.W. Andreasen, A simple nanostructured polymer/ZnO hybrid solar cell—preparation and operation in air, Nanotechnology 19 (2008) 424013–424025.
[132] F.C. Krebs, Air stable polymer photovoltaics based on a process free from vacuum steps and fullerenes, Sol. Energy Mater. Sol. Cells 92 (2008) 715–726.
[133] S.A. Gevorgyan, F.C. Krebs, Bulk heterojunctions based on native polythiophene, Chem. Mater. 20 (2008) 4386–4390.
[134] M. Jerring, J.S. Nielsen, N.C. Nielsen, F.C. Krebs, Polythiophene by Solution Processing, Macromolecules 40 (2007) 6012–6013.
135 M.H. Petersen, S.A. Gevorgyan, F.C. Krebs, Thermocleavable low band gap polymers and solar cells therefrom with remarkable stability toward oxygen, Macromolecules 41 (2008) 8986–8994.
[136] H. Neugebauer, C. Brabec, J.C. Hummelen, N.S. Sariciftci, Stability and photodegradation mechanisms of conjugated polymer/fullerene plastic solar cells, Sol. Energy Mater. Sol. Cells 61 (2000) 35–42.
[137] A. Gadisa, K. Tvingstedt, S. Admassie, L. Lindell, X. Crispin, M.R. Andersson, W.R. Salaneck, Olle Inganäs, Transparent polymer cathode for organic photovoltaic devices, Synth. Met. 156 (2006) 1102–1107.
[138] F.C.Krebs Winther-Jensen, High-conductivity large-area semi-transparent electrodes for polymer photovoltaics by silk screen printing and vapour-phase deposition, Sol. Energy Mater. Sol. Cells 90 (2006) 123–132.
[139] K. Myung-Gyu, G.L. Jay, Nanoimprinted semitransparent metal electrodes and their application in organic light-emitting diodes, Adv. Mater. 19 (2007) 1391–1396.
[140] Z. Wu, Z. Chen, X. Du, J.M. Lgan, J. Sippel, M. Nikolou, K. Kamaras, J.R. Reynolds, D.B Tanner, A.F Hebard, A.G Rinzler, Transparent conductive carbon nanotube films, Science 305 (2004) 1273–1276.
[141] T. Aernouts, P. Vanlaeke, W. Geens, J. Poortmans, P. Heremans, S. Borghs, R. Mertens, R. Andriessen, L. Leenders, Printable anodes for flexible organic solar cell modules, Thin Solid Films 451-452 (2004) 22–25.
[142] K. Tvingstedt, O. Inganäs, Electrode grids for ITO-free organic photovoltaic devices, Adv. Mater. 19 (2007) 2893–2897.
[143] J.Y. Lee, S.T. Connor, Y. Cui, P. Peumans, Solution-processed metal nanowire mesh transparent electrodes, Nano Lett. 8 (2008) 689–692.
[144] B. Zimmermann, M. Glatthaar, M. Niggemann, M.K. Riede, A. Hinsch, A. Gombert, ITO-free wrap through organic solar cells—a module concept for cost-efficient reel-to-reel production, Sol. Energy Mater. Sol. Cells 91 (2007) 374–378.
[145] M. Strange, D. Plackett, M. Kaasgaard, F.C. Krebs, Biodegradable polymer solar cells, Sol. Energy Mater. Sol. Cells 92 (2008) 805–813.
[146] F.C. Krebs, M. Jørgensen, K. Norrman, O. Hagemann, J. Alstrup, T.D. Nielsen, J. Fyenbo, K. Larsen, J. Kristensen, A complete process for production of flexible large area polymer solar cells entirely using screen printing—first publicde monstration, Sol. Energy Mater. Sol. Cells 93 (2009) 422–441.
[147] F.C. Krebs, H. Spanggard, T. Kjær, M. Biancardo, J. Alstrup, Large area plastic solar cell modules, Mater. Sci. Eng. B 138 (2007) 106–111.
[148] F.C. Krebs, J. Alstrup, H. Spanggaard, K. Larsen, E. Kold, Production of large-area polymer solar cells by industrial silk screen printing, lifetime considerations and lamination with polyethyleneterephthalate, Sol. Energy Mater. Sol. Cells 83 (2004) 293–300.
[149] F.C. Krebs, Roll-to-roll fabrication of monolithic large-area polymer solar cells free from indium-tin-oxide, Sol. Energy Mater. Sol. Cells 93 (2009) 1636–1641.
[150] F.C. Krebs, Polymer solar cell modules prepared using roll-to-roll methods: knife-over-edge coating, slot-die coating and screen printing, Sol. Energy Mater. Sol. Cells 93 (2009) 465–475.
[151] F.C. Krebs, All solution roll-to-roll processed polymer solar cells free from indium-tin-oxide and vacuum coating steps, Org. Electron. 10 (2009) 761–768.
[152] M. Niggemann, B. Zimmermann, J. Haschke, M. Glatthaar, A. Gombert, Organic solar cell modules for specific applications—from energy autonomous systems to large area photovoltaics, Thin Solid Films 516 (2008) 7181–7187.
[153] C. Lungenschmied, G. Dennler, H. Neugebauer, S.N. Sariciftci, M. Glatthaar, T. Meyer, A. Meyer, Flexible, long-lived, large-area, organic solar cells, Sol. Energy Mater. Sol. Cells 91 (2007) 379–384.
[154] S.E. Shaheen, R. Radspinner, N. Peyghambarian, G.E. Jabbour, Fabrication of bulk heterojunction plastic solar cells by screen printing, Appl. Phys. Lett. 79 (2001) 2996–2998.
[155] R. Tipnis, J. Bernkopf, S.J. Jia, J. Krieg, S. Li, M. Storch, D. Laird, Large-area organic photovoltaic module—fabrication and performance, Sol. Energy Mater. Sol. Cells 93 (2009) 442–446.
[156] L. Blankenburg, K. Schultheis, H. Schache, S. Sensfuss, M. Schrödner, Reel-to-reel wet coating as an efficient up-scaling technique for the production of bulk-heterojunction polymer solar cells, Sol. Energy Mater. Sol. Cells 93 (2009) 476–483.
[157] F.C. Krebs, S.A. Gevorgyan, J. Alstrup, A roll-to-roll process to flexible polymer solar cells: model studies, manufacture and operational stability studies, J. Mater. Chem 19 (2009) 5442–5451.